

**Title:** A Pilot Study of  $^{68}\text{Ga}$ -PSMA11 and  $^{68}\text{Ga}$ -RM2 PET/MRI for Biopsy Guidance in Patients with Suspected Prostate Cancer

**Authors:** Heying Duan<sup>1</sup>, Pejman Ghanouni<sup>2</sup>, Bruce Daniel<sup>2</sup>, Jarrett Rosenberg<sup>1</sup>, Alan Thong<sup>3</sup>, Christian Kunder<sup>4</sup>, Carina Mari Aparici<sup>1</sup>, Guido A. Davidzon<sup>1</sup>, Farshad Moradi<sup>1</sup>, Geoffrey A. Sonn<sup>3</sup>, Andrei Iagaru<sup>1</sup>

**Author Affiliations:**

<sup>1</sup> Department of Radiology, Division of Nuclear Medicine and Molecular Imaging, Stanford University, Stanford, CA

<sup>2</sup> Department of Radiology, Division of Body MRI, Stanford University, Stanford, CA

<sup>3</sup> Department of Urology, Stanford University, Stanford, CA

<sup>4</sup> Department of Pathology, Stanford University, Stanford, CA

**First author:**

Heying Duan, MD (Research fellow), ORCID 0000-0002-2834-5524

Department of Radiology, Division of Nuclear Medicine and Molecular Imaging

Stanford University

300 Pasteur Drive, H2200

Stanford, CA 94305

Phone: +1 650 725 4711

Fax: +1 650 498 5047

heyding@stanford.edu

**Corresponding author:**

Andrei Iagaru, MD, ORCID 0000-0003-0839-5329

Department of Radiology, Division of Nuclear Medicine and Molecular Imaging

Stanford University

300 Pasteur Drive, H2200

Stanford, CA 94305

Phone: +1 650 725 4711

Fax: +1 650 498 5047

aiagaru@stanford.edu

**Word Count:** 5009

**Clinicaltrials.gov Identifier:** NCT03809078

**Financial Support:** The study was partially supported by GE Healthcare.

**Running Title:** PSMA and GRPR PET-guided Prostate Biopsy

## Abstract

**Purpose:** Targeting of lesions seen on multiparametric MRI (mpMRI) improves prostate cancer (PC) detection at biopsy. However, 20–65% of highly suspicious lesions on mpMRI (PI-RADS 4 or 5) are false positives (FP), while 5–10% of clinically significant PC (csPC) are missed. Prostate specific membrane antigen (PSMA) and gastrin-releasing peptide receptors (GRPR) are both overexpressed in PC. We therefore aimed to evaluate the potential of  $^{68}\text{Ga}$ -PSMA11 and  $^{68}\text{Ga}$ -RM2 PET/MRI for biopsy guidance in patients with suspected PC.

**Methods:** A highly selective cohort of 13 men, aged  $58.0 \pm 7.1$  years, with suspected PC (persistently high prostate-specific antigen [PSA] and PSA density) but negative or equivocal mpMRI and/or negative biopsy were prospectively enrolled to undergo  $^{68}\text{Ga}$ -PSMA11 and  $^{68}\text{Ga}$ -RM2 PET/MRI. PET/MRI included whole-body and dedicated pelvic imaging after a delay of 20 minutes. All patients had targeted biopsy of any lesions seen on PET followed by standard 12-core biopsy. Maximum standardized uptake values ( $\text{SUV}_{\text{max}}$ ) of suspected PC lesions were collected and compared to gold standard biopsy.

**Results:** PSA and PSA density at enrollment were  $9.8 \pm 6.0$  (1.5–25.5) ng/mL and  $0.20 \pm 0.18$  (0.06–0.68) ng/mL<sup>2</sup>, respectively. Standardized systematic biopsy revealed a total of 14 PC in 8 participants: 7 were csPC and 7 were non-clinically significant PC (ncsPC).  $^{68}\text{Ga}$ -PSMA11 identified 25 lesions, of which 11 (44%) were true positive (TP) (5 csPC).  $^{68}\text{Ga}$ -RM2 showed 27 lesions, of which 14 (52%) were TP, identifying all 7 csPC and also 7 ncsPC. There were 17 concordant lesions in 11 patients vs. 14 discordant lesions in 7 patients between  $^{68}\text{Ga}$ -PSMA11 and  $^{68}\text{Ga}$ -RM2 PET. Incongruent lesions had the highest rate of FP (12 FP vs. 2 TP).  $\text{SUV}_{\text{max}}$  was significantly higher for TP than FP lesions in delayed pelvic imaging for  $^{68}\text{Ga}$ -PSMA11 ( $6.49 \pm 4.14$  vs.  $4.05 \pm 1.55$ ,  $P=0.023$ ) but not for whole-body images, nor for  $^{68}\text{Ga}$ -RM2.

**Conclusion:** Our results show that  $^{68}\text{Ga}$ -PSMA11 and  $^{68}\text{Ga}$ -RM2 PET/MRI are feasible for biopsy guidance in suspected PC. Both radiopharmaceuticals detected additional clinically significant

cancers not seen on mpMRI in this selective cohort.  $^{68}\text{Ga}$ -RM2 PET/MRI identified all csPC confirmed at biopsy.

**Key words:**  $^{68}\text{Ga}$ -RM2;  $^{68}\text{Ga}$ -PSMA11; Biopsy guidance; PET/MRI; Prostate cancer

## Introduction

The most common pathway to diagnose prostate cancer (PC) is through prostate needle biopsy driven by high serum prostate-specific antigen (PSA). PSA is a highly sensitive but not very specific marker for PC. Therefore, relying solely on elevated PSA for prostate biopsy leads to unnecessary biopsies with negative results or over-diagnosing of non-clinically significant PC (ncsPC) (1). Transrectal ultrasound (TRUS) is widely available and used to guide prostate biopsies. It consists of systematic sampling of the entire prostate using 12 passes through the rectum or perineum. This standardized procedure can miss cancers located in the prostate anteriorly (2). Multiple trials showed that multiparametric magnetic resonance imaging (mpMRI)-guided prostate biopsy had higher accuracy in detecting clinically significant PC (csPC), i.e., Gleason score  $\geq 3+4$ , than TRUS (3-5). However, 20–65% of suspicious lesions on mpMRI (PI-RADS 4 or 5) are false positives (FP), while 5–10% of csPC may be missed by mpMRI (6-10). Like TRUS, mpMRI also has 'blind spots' in the transition and central zone of the prostate where PC lesions may be overlooked (11).

Positron emission tomography (PET) combined with MRI and prostate-specific membrane antigen (PSMA) targeting radiopharmaceuticals improved PC imaging significantly. However, PSMA-targeted compounds have certain limitations related to expression in other normal tissues and pathologies, while up to 10% of PC are PSMA-negative (12,13).  $^{68}\text{Ga}$ -RM2 is a PET radiopharmaceutical that targets gastrin releasing peptide receptors (GRPR) which are highly overexpressed in PC, while benign prostate tissues show lower expression (14). GRPR expression is particularly high at earlier stages of prostatic carcinogenesis, making it an interesting target for initial staging (15,16). PSMA and GRPR targeting radiotracer have been reported as complementary to each other (17,18).  $^{68}\text{Ga}$ -PSMA11 PET/computed tomography (CT) targeted prostate biopsy showed high accuracy of 80.6% (19) while  $^{68}\text{Ga}$ -PSMA11 PET/MRI with its high soft tissue contrast and various functional sequences performed better with an accuracy of 90% (20).

In this prospective pilot study, we aimed to evaluate the potential of combined  $^{68}\text{Ga}$ -PSMA11 and  $^{68}\text{Ga}$ -RM2 PET/MRI for biopsy guidance in a highly selective patient cohort who had prior negative or equivocal mpMRI (PI-RADS 1–3) and/or prior negative prostate biopsy but persistent elevated PSA and PSA density, therefore considered highly suspicious of having PC. We also assessed the potential for detection of csPC.

## **Materials And Methods**

### *Participants*

Participants with negative or equivocal mpMRI (PI-RADS 1–3) and/or prior negative prostate biopsy with clinically suspicion for PC, defined as persistently elevated and rising PSA and PSA density, were prospectively enrolled and underwent either  $^{68}\text{Ga}$ -PSMA11 PET/MRI first followed by  $^{68}\text{Ga}$ -RM2 PET/MRI within two weeks or vice versa. This prospective, open-label, HIPAA-compliant study was approved by the local institutional review board and was registered on ClinicalTrials.gov (NCT03809078). All patients provided written informed consent. The intended total number of participants was 20; however, the FDA approval for  $^{68}\text{Ga}$ -PSMA11 during the timeline of the protocol made funding and completion of planned enrollment unfeasible.

### *Scanning protocols*

#### *PET/MRI*

Imaging was performed using a 3T time-of-flight enabled PET/MRI scanner (SIGNA PET/MRI, GE Healthcare, Waukesha, WI, USA), as previously described (17,21). Image acquisition started at  $46\pm 3$  (40–51) minutes after injection of  $176\pm 39$  (81–208) MBq  $^{68}\text{Ga}$ -PSMA11, and at  $45\pm 3$  (40–49) minutes after injection of  $139\pm 9$  (116–155) MBq  $^{68}\text{Ga}$ -RM2. Simultaneous PET/MRI was acquired from vertex to mid-thigh with an acquisition time of 4 minutes per bed position. Additional dedicated 20-minute pelvic images were acquired after a delay of  $26\pm 6$  (19–41) minutes for  $^{68}\text{Ga}$ -PSMA11, and  $25\pm 6$  (13–38) minutes for  $^{68}\text{Ga}$ -RM2. The

PET/MRI scans were performed  $7\pm 3$  (2–12) days apart. Synthesis of  $^{68}\text{Ga}$ -PSMA11 and  $^{68}\text{Ga}$ -RM2 was previously described (17).

### *mpMRI*

Multiparametric MRI was performed as routine clinical scan before prostate biopsy using a 3T scanner (MR750, GE Healthcare, Waukesha, WI, USA) with an external 32-channel body array coil. The imaging protocol consisted of T2 weighted imaging (T2WI), diffusion weighted imaging (DWI), and dynamic contrast-enhanced (DCE) imaging sequences. DWI were obtained using a combination of b-values (b50/800/1400/calculated 2000 s/mm<sup>2</sup>). Detailed acquisition parameters were previously described (22).

### *Image Analysis*

Two nuclear medicine physicians reviewed and analyzed PET images independently and in random order. Any focal uptake of  $^{68}\text{Ga}$ -RM2 or  $^{68}\text{Ga}$ -PSMA11 with a maximum standardized uptake value ( $\text{SUV}_{\text{max}}$ ) above adjacent prostate background, and not associated with physiologic accumulation was recorded as suspicious for PC. A region of interest (ROI) was drawn over suspected lesions to measure  $\text{SUV}_{\text{max}}$  and peak SUV ( $\text{SUV}_{\text{peak}}$ ) and served as identification marker.  $\text{SUV}_{\text{peak}}$  is defined as the average SUV within a small, fixed-size region of interest (1 cm<sup>3</sup>) (23). The MR portion was used for anatomical and lesion (if any were seen) correlation. For segment-based sensitivity and specificity calculation, the prostate was divided into the same 12 segments as for systematic prostate biopsy on MR images.

mpMRI was analyzed using the Prostate Imaging-Reporting and Data System (PI-RADS) criteria, version 2 (24). Lesions with PI-RADS score  $\geq 3$  were recorded. A PI-RADS score of 3 was considered equivocal, PI-RADS of 4 likely, and PI-RADS 5 highly likely for PC.

### *Prostate biopsy*

Prostate biopsies were performed transrectally under peripheral nerve block anesthesia by a single urologist.  $^{68}\text{Ga}$ -RM2 and  $^{68}\text{Ga}$ -PSMA PET/MRI, and mpMRI were reviewed by the urologist, radiologist, and nuclear medicine physician. Any PET positive lesions were annotated on the correlating mpMRI. The transrectal ultrasound probe (Noblus, Hitachi Aloka, Wallingford, CT, USA) was attached to the robotic arm of a prostate fusion biopsy system (Eigen/Artemis, Grass Valley, CA, USA) which enabled registration and fusion of mpMRI with real-time ultrasound to create a 3D model of the prostate with delineated annotations. PET-guided biopsy included a maximum of three cores per target lesion. Next, systematic 12-core biopsy was obtained consisting of one core through the apex, mid, and base regions, both medially and laterally, from left and right prostate lobes (25,26).

### *Statistical Analysis*

Statistical analysis was performed using Stata 16.1 (StataCorp LP, College Station, TX, USA) and R version 4.1.1 (r-project.org). Continuous data are presented as median $\pm$ standard deviation (SD), minimum (min)–maximum (max) values. Sensitivity and specificity are given in percentage with 95% confidence interval (CI). A Student's *T*-test was used to assess significance between SUV of whole-body and delayed pelvic imaging. Comparison between biopsy-positive and biopsy-negative prostate segments for PI-RADS and SUV<sub>max</sub>, was done by Wilcoxon ranksum test adjusted for clustering.

### **Results**

Thirteen men, 58.0 $\pm$ 7.1-year-old (41.0–69.0) with suspected PC were prospectively enrolled. PSA and PSA density at the time of PET/MRI were 9.8 $\pm$ 6.0 (1.5–25.5) ng/mL and 0.20 $\pm$ 0.18 (0.06–0.68) ng/mL<sup>2</sup>, respectively. Prostate biopsy prior to imaging was available in



12/13 patients of which 9 were negative and 3 showed Gleason 3+4 cancer (negative mpMRI). All patients' characteristics are summarized in Table 1.

### *mpMRI*

All participants underwent routine pre-biopsy mpMRI: 5 had a negative scan while 10 lesions were seen in 8 participants. There were three PI-RADS 3 (equivocal), six PI-RADS 4 and one PI-RADS 5 lesions. At study enrollment, four of the PI-RADS 4 lesions had negative prostate biopsies while two PI-RADS 4 and the one PI-RADS 5 lesion were equivocal on prior mpMRI from outside institutions (Table 1). Biopsy confirmed 3 true negative (TN) participants, 6 true positive (TP) lesions of which all were csPC, and 4 FP lesions. The highest number of false negatives (FN) was seen in mpMRI with 9; however, only 2 FN were csPC. Sensitivity and specificity were 30% (95% CI: 5, 77%) and 95% (95% CI: 85, 98%), respectively.

### *Prostate biopsy*

Prostate biopsies were performed  $19 \pm 12$  (2–38) days after PET/MRI. A median of  $8 \pm 3$  (2–13) additional PET-guided biopsies were performed in addition to systematic 12-core template. One patient refused to undergo systematic biopsy and had PET-guided biopsy only. Histopathology showed PC in 8/13 (61.5%) patients with a total of 14 PC lesions (multifocal disease in 6 patients) of which 7 (50%) were csPC. Standard template prostate biopsy found 6/14 (42.9%) PC of which 2 were csPC. PET-guided biopsy identified 8/14 (57.1%) PC lesions of which 5 were csPC. Standard template biopsy was negative in one patient for whom both  $^{68}\text{Ga}$ -RM2 and  $^{68}\text{Ga}$ -PSMA PET-guided biopsy showed Gleason 3+4 cancer.

### *$^{68}\text{Ga}$ -PSMA11 PET/MRI*

$^{68}\text{Ga}$ -PSMA11 PET/MRI found 25 intraprostatic lesions in the 13 participants (Figure 1).  $\text{SUV}_{\text{max}}$  decreased significantly from the whole-body to the dedicated pelvic images, but all lesions

were identified at both time points. Biopsy confirmed 11 PC lesions of which 5 were csPC, 14 FP, and 2 FN (both csPC).  $SUV_{max}$  of TP lesions were significantly higher than FP on the delayed pelvic but not on whole-body images. No other statistically significant differences were observed between  $SUV_{max}$  and  $SUV_{peak}$  for  $^{68}Ga$ -PSMA11 PET/MRI, including comparison of csPC and ncsPC. SUV measurements are summarized in Table 2. Sensitivity and specificity were 63% (95% CI: 19, 92%) and 83% (95% CI: 73, 94%), respectively.

### *$^{68}Ga$ -RM2 PET/MRI*

$^{68}Ga$ -RM2 PET/MRI showed 27 intraprostatic lesions in 12/13 participants. The participant with negative  $^{68}Ga$ -RM2 PET had negative prostate biopsies and was considered TN as cancer of unknown primary was found (FP in  $^{68}Ga$ -PSMA11 PET). No statistically significant changes were found between  $SUV_{max}$  and  $SUV_{peak}$  from whole-body and delayed pelvic images.  $^{68}Ga$ -RM2 PET detected all lesions identified on standard and PET-guided biopsy (14 TP of which 7 were csPC and 7 ncsPC). There were 13 FP on  $^{68}Ga$ -RM2 of which 12 were the same lesions as on  $^{68}Ga$ -PSMA11. When comparing  $SUV_{max}$  and  $SUV_{peak}$  of TP and FP lesions, no statistically significant changes were found on whole-body or delayed pelvic images (Table 2). Sensitivity was 83% (95% CI: 40, 97%), while specificity was 67% (95% CI: 40, 86%).

### *Comparison between $^{68}Ga$ -PSMA11 and $^{68}Ga$ -RM2*

Concordance between both radiopharmaceuticals was seen in 17 lesions in 11 participants. Of these, 11 lesions were PC with 6 being csPC (Supplemental Figure 1). Non-congruent uptake was observed in 14 lesions in 7 patients. Amongst these, 3 were PC with 1 csPC seen on  $^{68}Ga$ -RM2 (Supplemental Figure 2), while 10 were FP ( $^{68}Ga$ -PSMA11 and  $^{68}Ga$ -RM2 each had 5 FP). In 3 patients, a difference in intensity of tracer uptake was observed (Figure 2). Table 3 gives a semi-quantitative measurement (target tumor to normal prostate ratio) of lesions for  $^{68}Ga$ -PSMA11 and  $^{68}Ga$ -RM2 PET.

No lymph node or other distant metastases were identified on <sup>68</sup>Ga-PSMA11 or <sup>68</sup>Ga-RM2 PET/MRI.

## **Discussion**

In this pilot study, we evaluated the utility of <sup>68</sup>Ga-PSMA11 and <sup>68</sup>Ga-RM2 PET/MRI for prostate biopsy guidance in men with suspected PC but negative/equivocal mpMRI and/or negative prostate biopsy. In this small cohort, PET-guided biopsy detected more PC lesions than systematic 12-core biopsy, which was not surprising given the plethora of work showing the superiority of mpMRI-guided over standard biopsy (3,4,8). When compared to mpMRI, PET-guided biopsy not only found more TP lesions, but more importantly, more csPC.

A recently published study explored <sup>68</sup>Ga-PSMA617 and <sup>68</sup>Ga-RM26 PET/CT for biopsy guidance in 112 men with suspected PC (27). Of these participants, 35% had csPC and 4% ncsPC. Dual-tracer PET/CT-guided biopsy showed the highest detection rate without misdiagnosis of csPC (77%), followed by <sup>68</sup>Ga-PSMA617 (70%), <sup>68</sup>Ga-RM26 (56%), and mpMRI (36%). Despite the small number of participants and selective cohort, we identified a higher percentage of csPC (7/14 lesions, 50%) and ncsPC (7/14 lesions, 50%). The overall high sensitivity for PET-guided biopsy was comparable with our study. However, we observed a higher sensitivity for <sup>68</sup>Ga-RM2 (83%) leading to the detection of all biopsy-verified csPC and ncsPC with a similar FP rate as <sup>68</sup>Ga-PSMA11. This might suggest that this specific subgroup of men with negative anatomical imaging despite persistent elevated PSA may have a different tumor biology. PSMA and GRPR expression have been reported as complementary (17,18) with GRPR showing particular overexpression in earlier stages of PC (15). Therefore, GRPR-targeting radiopharmaceuticals may be a suitable alternative for biopsy guidance in men with suspected PC.

<sup>68</sup>Ga-PSMA11 PET/MRI (sensitivity 96%, specificity 81%) showed better performance compared to PET/CT (sensitivity 100%, specificity 68%) for guiding prostate biopsy (19,20). In

this study, sensitivity for  $^{68}\text{Ga}$ -PSMA11 was slightly less at 63%, which might be related to the specific subgroup of patients; however, specificity was higher at 83%. These overall high rates for PET/MRI are certainly attributable to the high soft tissue contrast of MRI but also related to the vast experience in MRI-fusion biopsy. The opportunity of switching from MRI- to PET-fusion for targeted prostate biopsy enables improved detection rates of csPC, especially in cases where mpMRI is inconclusive as seen in this present study. As PET/MRI scanners are not ubiquitously available, software fusion of MRI and PET has shown to be feasible and increased sensitivity of index lesion identification (28).

The PRIMARY trial investigated the added value of combining  $^{68}\text{Ga}$ -PSMA11 PET/CT with mpMRI for detecting csPC in men undergoing initial biopsy for suspected PC (29,30). Interestingly, all men with  $\text{SUV}_{\text{max}} \geq 12$  on  $^{68}\text{Ga}$ -PSMA11 PET had csPC at biopsy, independent of mpMRI results. In cases of PI-RADS  $\geq 4$ , an  $\text{SUV}_{\text{max}} \geq 9$  showed 100% specificity and positive predictive value in csPC detection. In our study, median  $\text{SUV}_{\text{max}}$  for csPC on  $^{68}\text{Ga}$ -PSMA11 PET was 7. This again could indicate a different tumor biology and expression pattern of PSMA in this specific subgroup of patients or differences in imaging technique.

$\text{SUV}_{\text{max}}$  from  $^{68}\text{Ga}$ -RM2 PET were higher than  $^{68}\text{Ga}$ -PSMA11, but so was the standard deviation for csPC and ncsPC, resulting in no significant differences. Despite earlier reports that GRPR expression is low to none in benign prostatic hyperplasia (BPH) (14,15), we observed uptake in BPH nodules.

We chose to additionally measure  $\text{SUV}_{\text{peak}}$  as  $\text{SUV}_{\text{max}}$  is a single pixel value that might be impacted by noise (31,32).  $\text{SUV}_{\text{peak}}$  may be a more robust quantitative measure due to its larger volume (23,33). We did not find any significant differences in  $\text{SUV}_{\text{peak}}$  between TP and FP lesions or csPC and ncsPC for  $^{68}\text{Ga}$ -PSMA11 or  $^{68}\text{Ga}$ -RM2.  $\text{SUV}_{\text{peak}}$  might be a more suitable measure for assessment of treatment response than single timepoint measurements (34).

Prostate biopsy bears an array of risks such as hematuria, rectal bleeding, infection, and pain (35,36). It is critical to identify the patients who will benefit from biopsy and distinguish csPC

from indolent cancers. An area of unmet need are men whose mpMRI are negative or equivocal but have a high suspicion for PC. These patients usually undergo serial imaging procedures, even multiple biopsies to find the source of their elevated PSA. Our results indicate that a combined approach of  $^{68}\text{Ga}$ -RM2 and  $^{68}\text{Ga}$ -PSMA11 PET/MRI has high sensitivity and specificity in localizing csPC and may help the urologist making subsequent treatment decisions. The higher upfront cost of such an approach may be cost-effective when compared to subsequent costs in its absence. This needs to be validated in larger studies.

The limitations of this study include the small number of participants, although this is common for pilot studies, and the highly selected patient cohort. However, the latter may be a positive differentiator for the use of PET/MRI in this clinical scenario. The sequence of biopsies performed – PET-guided prostate biopsy first, followed by standard template biopsy – might have affected the results of standard template biopsy due to swelling, bleeding, and tissue distortion.

## **Conclusion**

$^{68}\text{Ga}$ -PSMA11 and  $^{68}\text{Ga}$ -RM2 PET/MRI are feasible for biopsy guidance in men with suspected PC despite negative or equivocal mpMRI. Both radiopharmaceuticals detected additional csPC not seen on mpMRI.  $^{68}\text{Ga}$ -RM2 identified all csPC and ncsPC confirmed at biopsy. The incongruent uptake pattern for  $^{68}\text{Ga}$ -PSMA11 and  $^{68}\text{Ga}$ -RM2 reflect their different biological targets and expression. Larger studies are needed to shed light on their respective expression pattern at various stages of PC, as well as to guide future clinical use.

## **Financial Disclosure**

The study was partially supported by GE Healthcare.

## **Disclaimer**

All authors declare that they have no conflict or competing of interest.

## **Key Points**

**QUESTION:** Are  $^{68}\text{Ga}$ -PSMA11 and  $^{68}\text{Ga}$ -RM2 PET/MRI useful tools for guiding prostate biopsies in patients with suspected prostate cancer despite negative or equivocal mpMRI?

**PERTINENT FINDINGS:**  $^{68}\text{Ga}$ -PSMA11- and  $^{68}\text{Ga}$ -RM2-guided prostate biopsy led to detection of additional csPC not seen on mpMRI in this selective cohort of patients with prior negative or equivocal mpMRI and/or negative prostate biopsy but persistently elevated PSA and PSA density.  $^{68}\text{Ga}$ -RM2 PET/MRI accurately identified all csPC and ncsPC confirmed at biopsy.

**IMPLICATIONS FOR PATIENT CARE:**  $^{68}\text{Ga}$ -PSMA11- and  $^{68}\text{Ga}$ -RM2-guided prostate biopsy help detecting csPC and might therefore avoid unnecessary biopsies and associated risks.

## References

1. Brooks JD. Managing localized prostate cancer in the era of prostate-specific antigen screening. *Cancer*. 2013;119:3906-3909.
2. Mottet N, Bellmunt J, Bolla M, et al. EAU-ESTRO-SIOG Guidelines on Prostate Cancer. Part 1: Screening, Diagnosis, and Local Treatment with Curative Intent. *Eur Urol*. 2017;71:618-629.
3. Ahmed HU, El-Shater Bosaily A, Brown LC, et al. Diagnostic accuracy of multi-parametric MRI and TRUS biopsy in prostate cancer (PROMIS): a paired validating confirmatory study. *Lancet*. 2017;389:815-822.
4. Kasivisvanathan V, Rannikko AS, Borghi M, et al. MRI-Targeted or Standard Biopsy for Prostate-Cancer Diagnosis. *N Engl J Med*. 2018;378:1767-1777.
5. Ahdoot M, Wilbur AR, Reese SE, et al. MRI-Targeted, Systematic, and Combined Biopsy for Prostate Cancer Diagnosis. *N Engl J Med*. 2020;382:917-928.
6. Le JD, Tan N, Shkolyar E, et al. Multifocality and prostate cancer detection by multiparametric magnetic resonance imaging: correlation with whole-mount histopathology. *Eur Urol*. 2015;67:569-576.
7. Rouviere O, Puech P, Renard-Penna R, et al. Use of prostate systematic and targeted biopsy on the basis of multiparametric MRI in biopsy-naive patients (MRI-FIRST): a prospective, multicentre, paired diagnostic study. *Lancet Oncol*. 2019;20:100-109.
8. van der Leest M, Cornel E, Israel B, et al. Head-to-head Comparison of Transrectal Ultrasound-guided Prostate Biopsy Versus Multiparametric Prostate Resonance Imaging with Subsequent Magnetic Resonance-guided Biopsy in Biopsy-naive Men with Elevated Prostate-specific Antigen: A Large Prospective Multicenter Clinical Study. *Eur Urol*. 2019;75:570-578.
9. Truong M, Hollenberg G, Weinberg E, Messing EM, Miyamoto H, Frye TP. Impact of Gleason Subtype on Prostate Cancer Detection Using Multiparametric Magnetic Resonance Imaging: Correlation with Final Histopathology. *J Urol*. 2017;198:316-321.
10. Johnson DC, Raman SS, Mirak SA, et al. Detection of Individual Prostate Cancer Foci via Multiparametric Magnetic Resonance Imaging. *Eur Urol*. 2019;75:712-720.
11. Helfrich O, Puech P, Betrouni N, et al. Quantified analysis of histological components and architectural patterns of gleason grades in apparent diffusion coefficient restricted areas upon diffusion weighted MRI for peripheral or transition zone cancer locations. *J Magn Reson Imaging*. 2017;46:1786-1796.
12. Minner S, Wittmer C, Graefen M, et al. High level PSMA expression is associated with early PSA recurrence in surgically treated prostate cancer. *Prostate*. 2011;71:281-288.
13. Maurer T, Gschwend JE, Rauscher I, et al. Diagnostic Efficacy of (68)Gallium-PSMA Positron Emission Tomography Compared to Conventional Imaging for Lymph Node Staging of 130 Consecutive Patients with Intermediate to High Risk Prostate Cancer. *J Urol*. 2016;195:1436-1443.

14. Accardo A, Galli F, Mansi R, et al. Pre-clinical evaluation of eight DOTA coupled gastrin-releasing peptide receptor (GRP-R) ligands for in vivo targeting of receptor-expressing tumors. *EJNMMI Res.* 2016;6:17.
15. Korner M, Waser B, Rehmann R, Reubi JC. Early over-expression of GRP receptors in prostatic carcinogenesis. *Prostate.* 2014;74:217-224.
16. Duan H, Baratto L, Fan RE, et al. Correlation of (68)Ga-RM2 PET with Post-Surgery Histopathology Findings in Patients with Newly Diagnosed Intermediate- or High-Risk Prostate Cancer. *J Nucl Med.* 2022.
17. Minamimoto R, Sonni I, Hancock S, et al. Prospective Evaluation of (68)Ga-RM2 PET/MRI in Patients with Biochemical Recurrence of Prostate Cancer and Negative Findings on Conventional Imaging. *J Nucl Med.* 2018;59:803-808.
18. Touijer KA, Michaud L, Alvarez HAV, et al. Prospective Study of the Radiolabeled GRPR Antagonist BAY86-7548 for Positron Emission Tomography/Computed Tomography Imaging of Newly Diagnosed Prostate Cancer. *Eur Urol Oncol.* 2019;2:166-173.
19. Liu C, Liu T, Zhang Z, et al. (68)Ga-PSMA PET/CT Combined with PET/Ultrasound-Guided Prostate Biopsy Can Diagnose Clinically Significant Prostate Cancer in Men with Previous Negative Biopsy Results. *J Nucl Med.* 2020;61:1314-1319.
20. Ferraro DA, Becker AS, Kranzbuhler B, et al. Diagnostic performance of (68)Ga-PSMA-11 PET/MRI-guided biopsy in patients with suspected prostate cancer: a prospective single-center study. *Eur J Nucl Med Mol Imaging.* 2021;48:3315-3324.
21. Minamimoto R, Hancock S, Schneider B, et al. Pilot Comparison of (6)(8)Ga-RM2 PET and (6)(8)Ga-PSMA-11 PET in Patients with Biochemically Recurrent Prostate Cancer. *J Nucl Med.* 2016;57:557-562.
22. Sonn GA, Fan RE, Ghanouni P, et al. Prostate Magnetic Resonance Imaging Interpretation Varies Substantially Across Radiologists. *Eur Urol Focus.* 2019;5:592-599.
23. Wahl RL, Jacene H, Kasamon Y, Lodge MA. From RECIST to PERCIST: Evolving Considerations for PET response criteria in solid tumors. *J Nucl Med.* 2009;50 Suppl 1:122S-150S.
24. Weinreb JC, Barentsz JO, Choyke PL, et al. PI-RADS Prostate Imaging - Reporting and Data System: 2015, Version 2. *Eur Urol.* 2016;69:16-40.
25. Heidenreich A, Bastian PJ, Bellmunt J, et al. EAU guidelines on prostate cancer. part 1: screening, diagnosis, and local treatment with curative intent-update 2013. *Eur Urol.* 2014;65:124-137.
26. Wolf AM, Wender RC, Etzioni RB, et al. American Cancer Society guideline for the early detection of prostate cancer: update 2010. *CA Cancer J Clin.* 2010;60:70-98.



27. Qiu DX, Li J, Zhang JW, et al. Dual-tracer PET/CT-targeted, mpMRI-targeted, systematic biopsy, and combined biopsy for the diagnosis of prostate cancer: a pilot study. *Eur J Nucl Med Mol Imaging*. 2021.
28. Arslan A, Karaarslan E, Guner AL, et al. Comparison of MRI, PSMA PET/CT, and Fusion PSMA PET/MRI for Detection of Clinically Significant Prostate Cancer. *J Comput Assist Tomogr*. 2021;45:210-217.
29. Amin A, Blazevski A, Thompson J, et al. Protocol for the PRIMARY clinical trial, a prospective, multicentre, cross-sectional study of the additive diagnostic value of gallium-68 prostate-specific membrane antigen positron-emission tomography/computed tomography to multiparametric magnetic resonance imaging in the diagnostic setting for men being investigated for prostate cancer. *BJU Int*. 2020;125:515-524.
30. Emmett L, Buteau J, Papa N, et al. The Additive Diagnostic Value of Prostate-specific Membrane Antigen Positron Emission Tomography Computed Tomography to Multiparametric Magnetic Resonance Imaging Triage in the Diagnosis of Prostate Cancer (PRIMARY): A Prospective Multicentre Study. *Eur Urol*. 2021;80:682-689.
31. Boellaard R, Krak NC, Hoekstra OS, Lammertsma AA. Effects of noise, image resolution, and ROI definition on the accuracy of standard uptake values: a simulation study. *J Nucl Med*. 2004;45:1519-1527.
32. Laffon E, Lamare F, de Clermont H, Burger IA, Marthan R. Variability of average SUV from several hottest voxels is lower than that of SUVmax and SUVpeak. *Eur Radiol*. 2014;24:1964-1970.
33. Akamatsu G, Ikari Y, Nishida H, et al. Influence of Statistical Fluctuation on Reproducibility and Accuracy of SUVmax and SUVpeak: A Phantom Study. *J Nucl Med Technol*. 2015;43:222-226.
34. Vanderhoek M, Perlman SB, Jeraj R. Impact of the definition of peak standardized uptake value on quantification of treatment response. *J Nucl Med*. 2012;53:4-11.
35. Loeb S, Vellekoop A, Ahmed HU, et al. Systematic review of complications of prostate biopsy. *Eur Urol*. 2013;64:876-892.
36. Wagenlehner FM, van Oostrum E, Tenke P, et al. Infective complications after prostate biopsy: outcome of the Global Prevalence Study of Infections in Urology (GPIU) 2010 and 2011, a prospective multinational multicentre prostate biopsy study. *Eur Urol*. 2013;63:521-527.

Figures:

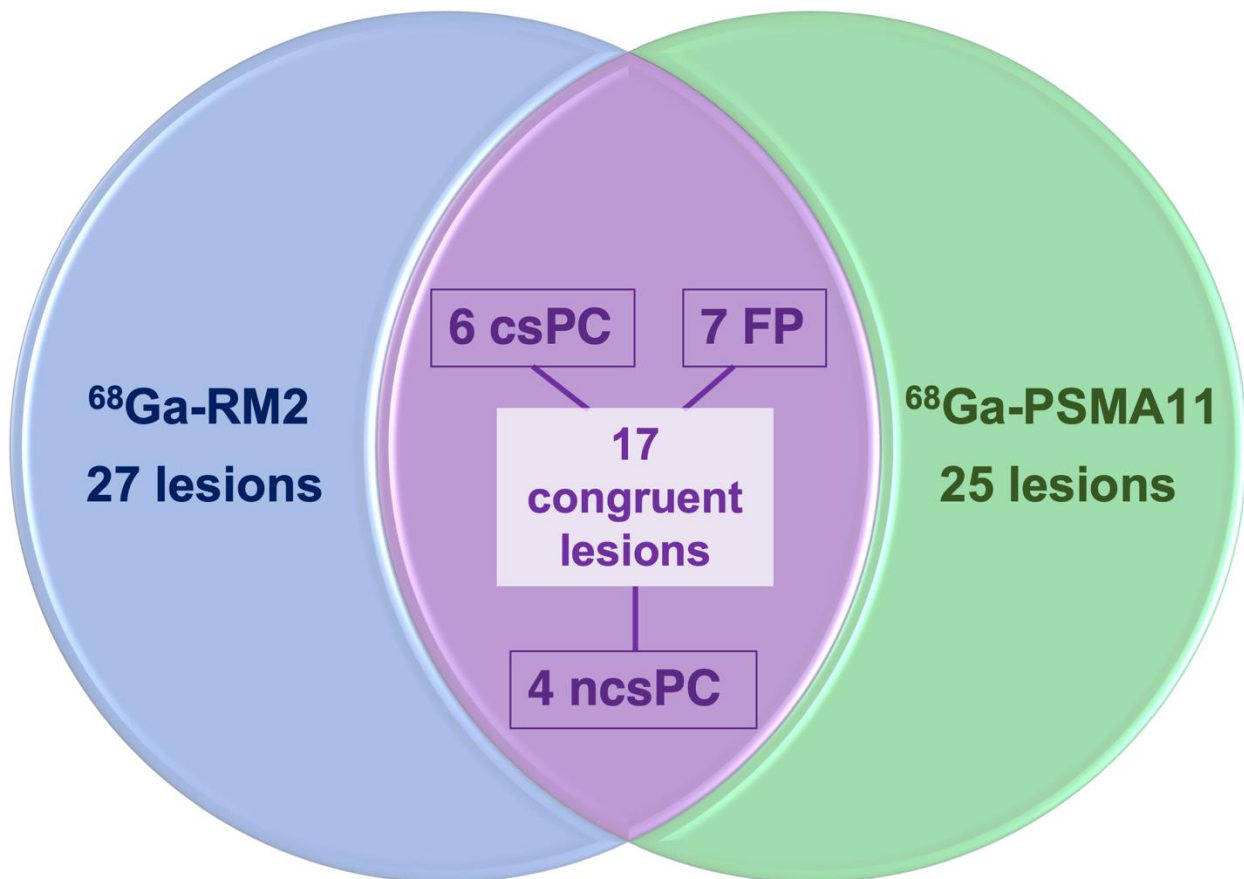


**Figure 1:** Venn diagram of  $^{68}\text{Ga}$ -PSMA11 and  $^{68}\text{Ga}$ -RM2 positivity with their congruent lesional uptake compared to biopsy results.

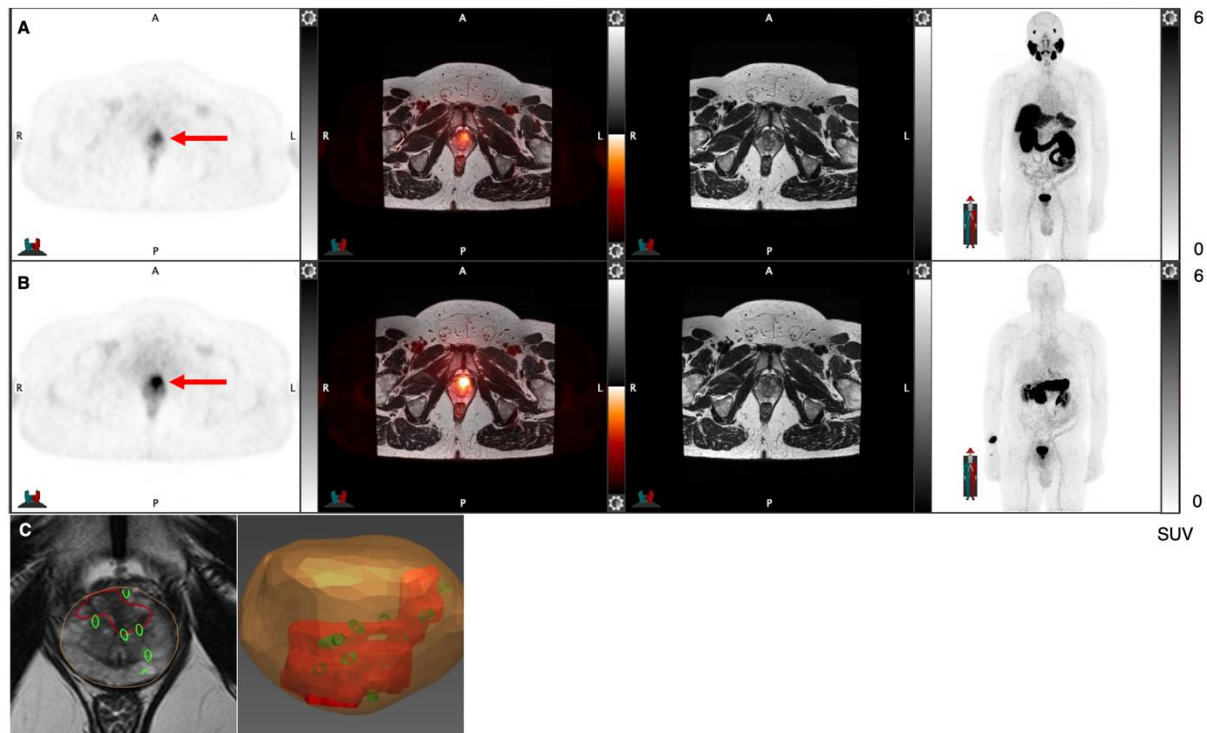


**Figure 2:** 58-year-old man presenting with PSA 12.8 ng/ml and PSA density 0.41 ng/ml<sup>2</sup>.  $^{68}\text{Ga}$ -RM2 (B, axial PET, fused PET/MRI, MRI, and MIP images) shows intense uptake in the anterior prostate (red arrows) while less pronounced on  $^{68}\text{Ga}$ -PSMA11 PET/MRI (A). PET-guided biopsy demonstrated Gleason 3+4 prostate cancer. Co-registration (C) of biopsy needle tracks in green, index tumor outlined in red on mpMRI as well as 3D-rendered image.

## Tables

**Table 1.** Patients' characteristics

<b><i>N</i></b>	13			
<b>Age (years)</b>	58.0 ± 7.1 (41.0 – 69.0)			
<b>PSA (ng/mL)</b>	9.8 ± 6.0 (1.5 – 25.5)			
<b>PSA density (ng/mL<sup>2</sup>)</b>	0.20 ± 0.18 (0.06 – 0.68)			
<b>Prior biopsy (<i>n</i>)</b>	12/13			
	Negative: 9/13		Gleason score 3+4: 3/13	
<b>Prior mpMRI (<i>n</i>)</b>	13/13			
	Negative: 6/13	PI-RADS 3: 3/13	PI-RADS 4: 4/13	PI-RADS 5: 0/13
	<b><sup>68</sup>Ga-PSMA11</b>		<b><sup>68</sup>Ga-RM2</b>	
<b>Injected activity (MBq)</b>	176 ± 39 (81 – 208)		139 ± 9 (116 – 155)	
<b>Uptake time (min)</b>	46 ± 3 (40 – 51)		45 ± 3 (40 – 49)	
<b>Delay time to pelvic PET/MRI (min)</b>	26 ± 6 (19 – 41)		25 ± 6 (13 – 38)	
<b>Time between scans (days)</b>	7 ± 3 (2 – 12)			

Numerical factors are expressed as median ± standard deviation (range).

**Table 2.** SUV<sub>max</sub> and SUV<sub>peak</sub> of all PET positive lesions, true positive and false positive lesions, and stratified to Gleason score at whole-body and delayed pelvic imaging for <sup>68</sup>Ga-PSMA11 and <sup>68</sup>Ga-RM2.

		<sup>68</sup> Ga-PSMA11		<sup>68</sup> Ga-RM2	
		Whole-body PET/MRI	Pelvic PET/MRI	Whole-body PET/MRI	Pelvic PET/MRI
All lesions	SUV <sub>max</sub>	4.56 ± 4.03 (3.20 – 22.46)	4.42 ± 3.27 (2.87 – 17.94)	9.10 ± 7.95 (4.31 – 40.15)	7.93 ± 9.49 (3.57 – 44.08)
	P-value	0.007		0.244	
	SUV <sub>peak</sub>	3.83 ± 2.03 (2.54 – 10.88)	3.60 ± 2.12 (2.27 – 10.80)	6.42 ± 5.68 (3.94 – 29.01)	6.06 ± 6.36 (3.00 – 31.95)
	P-value	0.072		0.163	
True positive	SUV <sub>max</sub>	6.57 ± 5.36 (3.98 – 22.46)	6.49 ± 4.14 (3.34 – 17.94)	8.64 ± 10.36 (4.31 – 40.15)	6.80 ± 12.34 (3.57 – 44.08)
	P-value	0.067	0.023	0.452	0.532
False positive	SUV <sub>max</sub>	4.54 ± 1.54 (3.20 – 7.99)	4.05 ± 1.55 (2.87 – 9.11)	9.69 ± 3.54 (5.18 – 16.99)	8.92 ± 4.50 (4.49 – 19.26)
True positive	SUV <sub>peak</sub>	4.35 ± 2.57 (2.84 – 10.88)	4.82 ± 2.65 (2.50 – 10.80)	6.11 ± 7.10 (3.94 – 29.01)	5.80 ± 8.14 (3.00 – 31.95)
	P-value	0.086	0.085	0.647	0.651
False positive	SUV <sub>peak</sub>	3.52 ± 1.15 (2.54 – 5.80)	3.43 ± 1.74 (2.27 – 9.56)	7.34 ± 3.48 (4.22 – 16.99)	6.92 ± 3.46 (3.94 – 15.71)
ncsPC	SUV <sub>max</sub>	5.42 ± 1.22 (4.06 – 7.66)	5.24 ± 1.87 (3.34 – 8.68)	8.16 ± 8.87 (5.96 – 34.18)	5.63 ± 12.67 (4.83 – 44.08)
	P-value	0.120	0.116	0.540	0.740
csPC	SUV <sub>max</sub>	6.96 ± 6.77 (3.98 – 22.46)	6.81 ± 4.90 (4.70 – 17.94)	10.56 ± 11.73 (4.31 – 40.15)	8.86 ± 11.74 (3.57 – 38.72)
ncsPC	SUV <sub>peak</sub>	3.99 ± 1.37 (2.84 – 6.05)	3.78 ± 1.86 (2.50 – 6.78)	5.79 ± 7.67 (4.75 – 29.01)	4.74 ± 8.96 (4.03 – 31.95)
	P-value	0.167	0.167	0.908	0.954
csPC	SUV <sub>peak</sub>	4.35 ± 3.06 (3.95 – 10.88)	4.82 ± 2.87 (4.18 – 10.80)	7.63 ± 6.26 (3.94 – 22.87)	6.10 ± 6.89 (3.00 – 23.83)

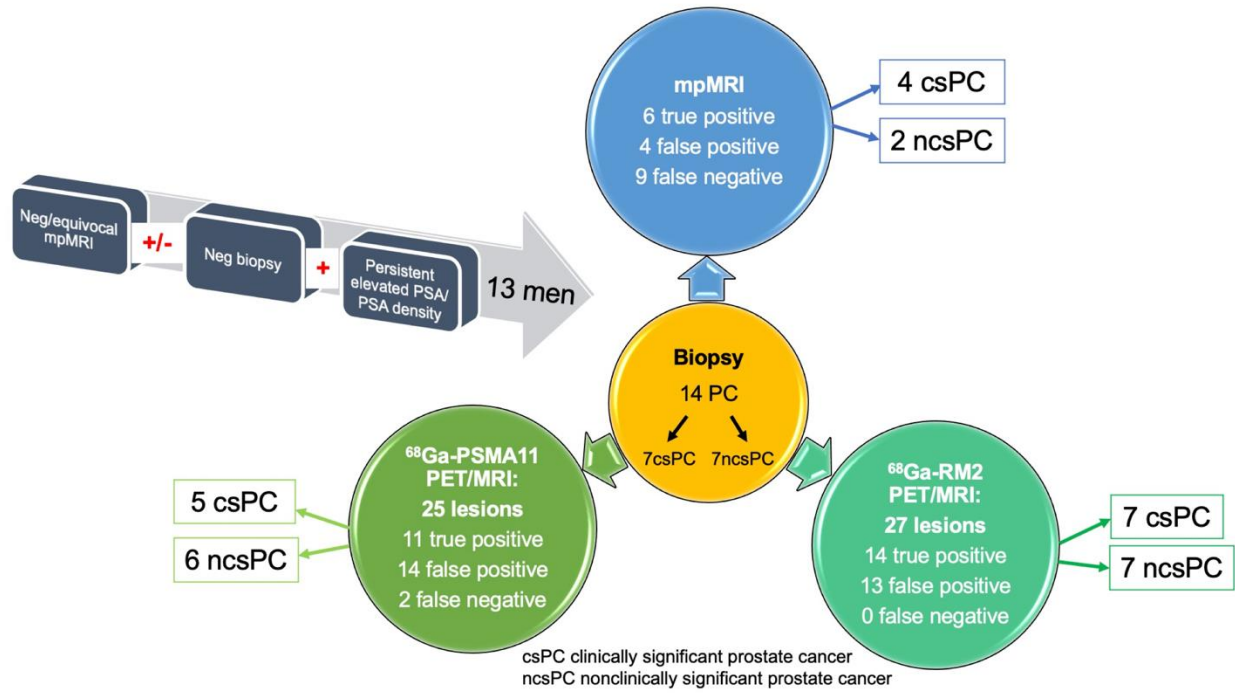
Numerical factors are expressed as median ± standard deviation (range).

**Table 3.** SUV<sub>max</sub> and SUV<sub>peak</sub> of all PET positive lesions, normal prostate tissue, and tumor-to-normal tissue-ratio (TNR) for whole-body and delayed pelvic imaging for <sup>68</sup>Ga-PSMA11 and <sup>68</sup>Ga-RM2.

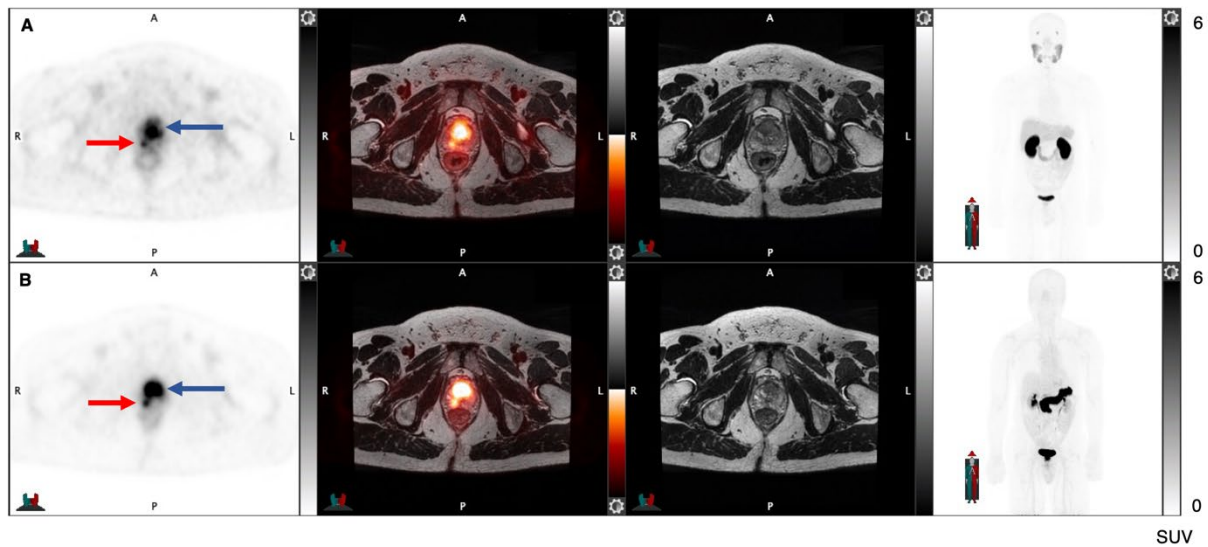
<b><sup>68</sup>Ga-PSMA11</b>						
	<b>SUV<sub>max</sub></b>			<b>SUV<sub>peak</sub></b>		
	<b>Prostate tumor</b>	<b>Normal prostate</b>	<b>TNR</b>	<b>Prostate tumor</b>	<b>Normal prostate</b>	<b>TNR</b>
<b>Whole-body PET/MRI</b>	4.56 ± 4.03 (3.20 – 22.46)	2.46 ± 0.45 (1.91 – 3.57)	2.23 ± 2.81 (1.51 – 11.76)	3.83 ± 2.03 (2.54 – 10.88)	2.61 ± 0.47 (2.01 – 3.63)	1.48 ± 1.21 (0.99 – 5.41)
<b>Pelvic PET/MRI</b>	4.42 ± 3.27 (2.87 – 17.94)	2.21 ± 0.29 (1.88 – 2.91)	2.39 ± 1.96 (1.36 – 8.50)	3.60 ± 2.12 (2.27 – 10.80)	2.37 ± 0.43 (1.62 – 3.27)	1.82 ± 1.52 (1.12 – 6.67)
<b><sup>68</sup>Ga-RM2</b>						
	<b>SUV<sub>max</sub></b>			<b>SUV<sub>peak</sub></b>		
	<b>Prostate tumor</b>	<b>Normal prostate</b>	<b>TNR</b>	<b>Prostate tumor</b>	<b>Normal prostate</b>	<b>TNR</b>
<b>Whole-body PET/MRI</b>	9.10 ± 7.95 (4.31 – 40.15)	3.25 ± 0.86 (2.10 – 5.66)	2.77 ± 4.87 (1.32 – 19.12)	6.42 ± 5.68 (3.94 – 29.01)	3.26 ± 0.73 (2.54 – 5.29)	2.36 ± 2.49 (1.21 – 8.87)
<b>Pelvic PET/MRI</b>	7.93 ± 9.49 (3.57 – 44.08)	3.00 ± 0.78 (2.24 – 5.16)	2.52 ± 4.96 (1.59 – 17.49)	6.06 ± 6.36 (3.00 – 31.95)	3.34 ± 0.60 (2.47 – 4.46)	2.19 ± 3.33 (1.20 – 12.43)

Numerical factors are expressed as median ± standard deviation (range).

# Graphical Abstract

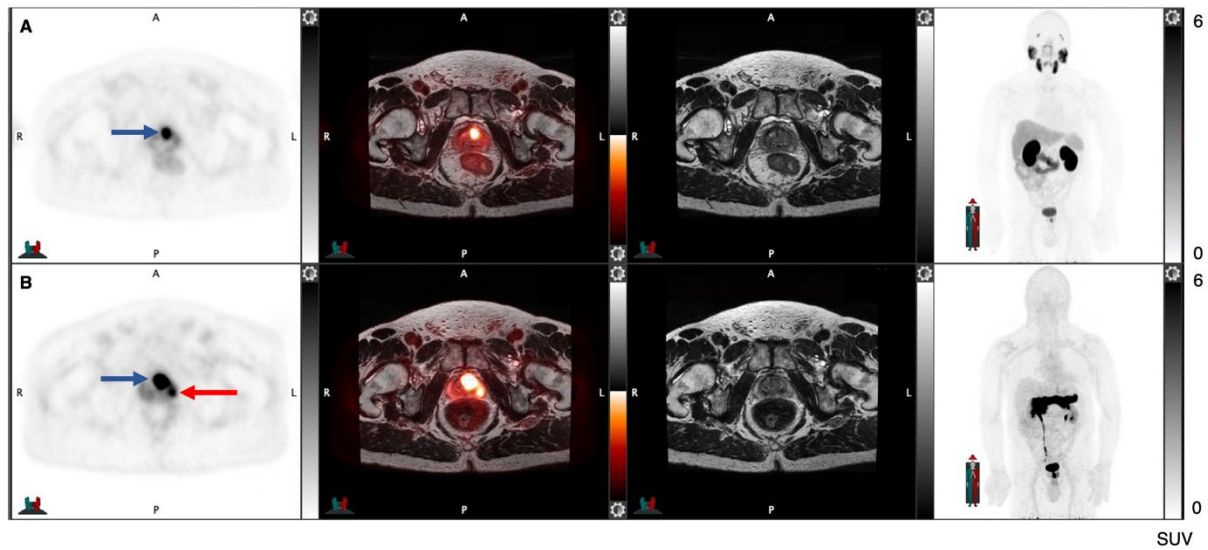


## Supplemental Figures



**Supplemental Figure 1:** 62-year-old man presenting with PSA 9.0 ng/mL and PSA density 0.24 ng/mL<sup>2</sup>. <sup>68</sup>Ga-PSMA11 (A, axial PET, fused PET/MRI, MRI, and maximum intensity projection [MIP] images) and <sup>68</sup>Ga-RM2 PET/MRI (B) show concordance of focal uptake anterior in the apex of the prostate (blue arrow) correlating to a Gleason 3+4 cancer and right medial (red arrow) corresponding to a Gleason 3+3 lesion.





**Supplemental Figure 2:** 69-year-old patient with prior equivocal mpMRI and negative prostate biopsy but persistent elevated PSA of 20.9 ng/mL and PSA density 0.68 ng/mL<sup>2</sup>. <sup>68</sup>Ga-PSMA11 (A, axial PET, fused PET/MRI, MRI, and MIP images) and <sup>68</sup>Ga-RM2 PET/MRI (B) show congruent focal uptake anterior in the apex of the prostate (blue arrow) correlating to Gleason 4+5 cancer. <sup>68</sup>Ga-RM2 identified additional uptake lateral left (red arrow) corresponding to a Gleason 3+3 lesion.